Published in final edited form as:
Science. 2012 August 31; 337(6098): 1072–1074. doi:10.1126/science.1224823.

Probing the Ultimate Limits of Plasmonic Enhancement

C. Ciracì[1,*], **R. T. Hill**[2], **J. J. Mock**[1], **Y. Urzhumov**[1], **A. I. Fernández-Domínguez**[3], **S. A. Maier**[3], **J. B. Pendry**[3], **A. Chilkoti**[2,4], and **D. R. Smith**[1]

[1]Center for Metamaterials and Integrated Plasmonics and Department of Electrical and Computer Engineering, Duke University, Durham, NC 27708, USA

[2]Center for Biologically Inspired Materials and Material Systems, Duke University, Durham, NC 27708, USA

[3]Department of Physics, The Blackett Laboratory, Imperial College London, London SW7 2AZ, UK

[4]Department of Biomedical Engineering, Duke University, Durham, NC 27708, USA

Abstract

Metals support surface plasmons at optical wavelengths and have the ability to localize light to sub-wavelength regions. The field enhancements that occur in these regions set the ultimate limitations on a wide range of nonlinear and quantum optical phenomena. Here we show that the dominant limiting factor is not the resistive loss of the metal, but the intrinsic nonlocality of its dielectric response. A semi-classical model of the electronic response of a metal places strict bounds on the ultimate field enhancement. We demonstrate the accuracy of this model by studying the optical scattering from gold nanoparticles spaced a few angstroms from a gold film. The bounds derived from the models and experiments impose limitations on all nanophotonic systems.

One of the most remarkable phenomena associated with metals at optical wavelengths is field enhancement. Local optical fields within a metal nanostructure can achieve strengths that are orders of magnitude greater than that of the incident field. This singular feature of metals serves as the fundamental mechanism for a host of radiative and scattering processes associated with nanophotonic systems. Field enhancement has been shown to impact surface-enhanced Raman scattering (1); nonlinear processes, such as enhanced harmonic generation (2) or wave mixing (3); nanolasing (4); plasmonic sensing (5); and enhancement of spontaneous emission (6).

The largest field enhancements in nanoplasmonic systems occur near sharp asperities or corners associated with metal nanoparticles (NPs) and within the sub-nanometer gaps formed between NP aggregates. An incident optical field drives currents across the NP, resulting in peak currents flowing through the NP during one part of the cycle, and a peak surface charge density during the other part of the cycle. Using the conventional, classical description of the metal's response—or local model—at the moment of peak polarization, the charges can be considered crushed into a layer of infinitesimal thickness along the NP surface, resulting in the standard surface charge density picture. Structures that possess a singularity, such as spheres that touch at a point, have been shown to possess continuous scattering spectra associated with compression of the surface plasmon wave field at the singularity. According to the local model, a pulse of surface plasmons launched into such a system would travel towards but never reach the singularity, giving rise to energy compression and enormous field enhancements (7).

*Correspondence to: cristian.ciraci@duke.edu.

It would appear, then, that virtually unbounded field enhancements should be possible, provided well-defined, sub-nanometer gaps could be created between nanostructures with sufficiently smooth surfaces. However in a real metal, polarization charge densities are not perfectly localized at a surface but are slightly spread over a thickness near the boundary. This dispersion of the charge effectively smoothes the singularities: charges no longer reside exactly at the surface, but acquire some volume as the charge density spreads into the NP. The scattering spectrum ceases to be continuous and is now discrete, with correspondingly reduced field enhancements (8, 9). These effects have long been recognized by theorists as witnessed by the early work of Fuchs and Claro (10) who showed that the nonlocal effects considered here limit the response of almost touching spheres.

The local model for free electron response inside metallic structures is insufficient to describe metals whose critical dimensions are on the order of a few nanometers or smaller. A more appropriate description should take into account atomic and sub-atomic interactions, particularly electron-electron repulsion. The Pauli exclusion principle forbids two fermions from occupying the same quantum state at a given time, resulting in a repulsive force between charge carriers. Along with the classical Coulomb force, the quantum repulsion manifests itself as a pressure in an electron gas that resists the compression induced by an applied electromagnetic field. This electron pressure may be taken into account by a hydrodynamic description of the collective motion of the electrons inside a metal (11). Neglecting nonlinear effects (12), we obtain the following equation for the currents **J** inside a metal:

$$\beta^2\nabla(\nabla\cdot\mathbf{J})+(\omega^2+i\gamma\omega)\mathbf{J}=i\omega\omega_p^2\varepsilon_0\mathbf{E}, \quad (1)$$

where γ and ω_P are the damping coefficient and the plasma frequency, respectively, which also appear in the conventional Drude formula, $\varepsilon(\omega)=1-\omega_p^2/(\omega^2-i\gamma\omega)$, and β — approximately the speed of sound in the Fermi-degenerate plasma of conduction electrons (11) — is proportional to the Fermi velocity ν_F.

The effect of including the pressure term in the electron response is that the longitudinal dielectric function, ε_L, becomes nonlocal, depending on the propagation vector in addition to the frequency, as follows:

$$\varepsilon_L(\mathbf{k},\omega)=1-\frac{\omega_p^2}{\omega^2+i\gamma\omega-\beta^2|\mathbf{k}|^2}, \quad (2)$$

while the transverse response is unchanged.

The simple picture, then, of a surface charge layer with infinitesimal extent must be replaced with a continuous charge density, whose extent will be determined by $\beta/\omega_P \propto \lambda_{TF}$, where $\lambda_{TF} = \nu_F/\omega_P$ is the Thomas-Fermi screening length. Rather than a strict surface charge density, the nonlocality produces a volume charge density that spreads out from the surface a distance roughly λ_{TF}, on the order of 1Å. As a result, the real behavior of the optical characteristics of sub-nanometer length systems may deviate from local model predictions (13).

A full quantum treatment of optical response is possible only for very small spheres. Therefore it is critical to develop and verify a semi-empirical model that can be applied to spheres of dimensions greater than a few nanometers. Here, we use the hydrodynamic model to take quantum effects into account, assuming that delocalization of surface charge is the dominant process. Alternative semi-empirical models have been developed that emphasize the tunneling current between two surfaces, which is present at very small separations (14–

16). We find that for the geometrical parameters of our experiments, the hydrodynamic model gives an excellent account of our data, though we concede that for smaller dimensions tunneling current may well play an important role.

To date, the experimental study of nonlocality on coupled plasmonic systems has been made hampered by the difficulty in reliably and precisely controlling sub-nanometer interparticle spacing. Even a relatively simple system, such as two nanospheres separated by a sub-nanometer gap, remains a challenge for colloidal or lithographic synthesis methods. By contrast, the closely related system of a metal nanosphere positioned a specified distance above a metallic film, is simple to fabricate and provides exquisite control of the spacing. The film-coupled nanosphere geometry (Fig. 1) involves the deposition of a metal film by standard sputtering or evaporation methodologies, followed by solution deposition of a molecular dielectric layer, and chemisorption of chemically synthesized metal NPs on the spacer layer.

As the NPs are brought closer to the film, the coupling between a given NP and its virtual image induces a red-shift in the peak of the plasmon resonance wavelength, which can be detected as the peak intensity in the measured scattering cross-section. Because the spacer layer exhibits tremendous uniformity, the scattering behavior of the NPs are remarkably uniform, and scattering measurements on a slide sample from ensembles of NPs are representative of the typical scattering of an individual film-coupled NP, as confirmed by dark-field microscopy. Numerical simulations reveal the expected behavior of strongly localized fields between the NP and film, related to the interaction of the NP with its electromagnetic image (Fig. 2). In addition, the field very near the surface of the metal sphere decays exponentially away from the surface on a scale given essentially by λ_{TF}.

The plasmon resonant scattering peak positions and enhancement factor for gap dimensions between 0.1 nm and 10 nm can be calculated using both the local model and the nonlocal model (Fig. 3). The plasmon resonance of the NP red-shifts predictably and the field enhancement grows as the gap dimension decreases. If the local model for the metal dielectric function is employed, the expected shift in the plasmon resonance wavelength is pushed to nearly $\lambda = 900$nm, corresponding to a peak local field enhancement of $\sim 10^4$ (Fig. 3). The presence of a nonzero β modifies the plasmon resonance wavelength shift, particularly significantly for separation distances below 5 nm. From 1 nm to 0.1 nm, the impact of the nonlocal electronic response is decisive, causing the peak resonance wavelength to occur at values much lower than that predicted by the local model. For the realistic value of the nonlocal parameter, $\beta = 1.0\times10^6$m/s— as expected from prior measurements and theory — the peak resonance wavelength shift is capped near 750 nm, a full 150 nm difference from that predicted using the local model. The impact of spreading the charge thus leads to dramatic optical shifts, easily measurable using spectroscopic techniques. Importantly, the field enhancement is still extremely large compared with the analogous 2D system (7), even with the nonlocal interactions taken into account. The expected enhancement exceeds values of 10^3 for realistic values of the parameter β (Fig. 3B). Far more than material losses, the nonlocality plays the dominant role in limiting electromagnetic enhancement of NPs, reducing the dimer or film-coupled NP peak enhancement by approximately a factor of four.

To experimentally test the validity of our predictions, precise control over extremely short gap lengths are required. We deposit spacer layers using either layer-by-layer (LBL) deposition of poly-electrolytes (5, 17, 18), for separations that range from 2.8 nm to 26.6 nm, or by the formation of self-assembled monolayers (SAMs) of amine-terminated alkanethiols for even smaller separation distances that range from 0.5 nm to 2.0 nm. We first prepare a set of 30 nm thick gold films; then incubate the gold films with either a series of

poly-electrolytes, or a set of amine-terminated alkanethiols wherein the gap length is tuned by the number of carbon atoms in the chain (Fig. 4A). The thicknesses of the SAM spacer layers have been estimated using a theoretical approach (12), as standard ellipsometry measurements have been shown before to produce systematically low thickness values for such thin SAMs on gold surfaces (19).

The optical response of the NPs deposited on the spacer layers is measured by illuminating the sample with white light and collecting the scattered light through a dark-field objective. The collected light is then directed through a 1 mm diameter image plane aperture to the spectrometer. The plasmon resonant scattering spectra for each of the samples—which correspond to different gap distances as determined by the chain length of the SAM—are shown in Fig. 4C. The results of both the local and nonlocal model simulations are plotted alongside the collected data in Fig. 4D, showing the plasmon resonance peak position dependence on film-NP gap distance. It was found that the electric permittivity of the spacer layer must be taken into account in the models to achieve the best fit. We used a non-dispersive index of refraction of $n = 1.8$. Comparison of the numerical simulations to our experimental results (Fig. 4D) reveals that the nonlocal model is in excellent agreement with the experimentally measured scattering peaks, confirming that the actual dielectric function is modified by the electron pressure term.

The agreement obtained demonstrates that the hydrodynamic model is a powerful tool that incorporates quantum effects in macroscopic systems, and shows that in certain cases the impact of nonlocality may prevail over purely quantum effects such as electron tunneling. Though direct measurements of near-field enhancement remain difficult at such scales, our results provide a strong experimental support in setting an upper limit to the maximum field enhancement achievable with plasmonic systems.

Supplementary Material

Refer to Web version on PubMed Central for supplementary material.

Acknowledgments

We are grateful to M. Scalora, S. Wolter, and A. Moreau for helpful input and discussion. This research was supported by the Air Force Office of Scientific Research (Grant No. FA9550-09-1-0562) and by the Army Research Office through a Multidisciplinary University Research Initiative (Grant No. W911NF-09-1-0539). J.B.P., S.A.M. and A.I.F.-D. gratefully acknowledge support from the Leverhulme Trust and the Marie Curie Actions. Additional support includes NIH grant R21EB009862 to A. C., and NIH F32 award (F32EB009299) to R.T.H.

References and Notes

1. Moskovits M. Surface-Enhanced Spectroscopy. Rev. Mod. Phys. 1985; 57:783–826.
2. Scalora M, et al. Second- and third-harmonic generation in metal-based structures. Phys. Rev. A. 2010; 82 043828.
3. Renger J, Quidant R, van Hulst N, Novotny L. Surface-Enhanced Nonlinear Four-Wave Mixing. Phys. Rev. Lett. 2010; 104 046803.
4. Oulton RF, et al. Plasmon lasers at deep subwavelength scale. Nature. 2009; 461:629–632. [PubMed: 19718019]
5. Mock JJ, Hill RT, Tsai Y-J, Chilkoti A, Smith DR. Probing Dynamically Tunable Localized Surface Plasmon Resonances of Film-Coupled Nanoparticles by Evanescent Wave Excitation. Nano Lett. 2012; 12:1757–1764. [PubMed: 22429053]
6. Gu Y, et al. Surface-Plasmon-Induced Modification on the Spontaneous Emission Spectrum via Subwavelength-Confined Anisotropic Purcell Factor. Nano Lett. 2012; 12:2488–2493. [PubMed: 22512860]

7. Fernández-Domínguez AI, Maier SA, Pendry JB. Collection and Concentration of Light by Touching Spheres: A Transformation Optics Approach. Phys. Rev. Lett. 2010; 105:266807. [PubMed: 21231703]
8. Fernández-Domínguez AI, Wiener A, Garcia-Vidal F, Maier SA, Pendry J. Transformation-Optics Description of Nonlocal Effects in Plasmonic Nanostructures. Phys. Rev. Lett. 2012; 108:106802. [PubMed: 22463438]
9. David C, García de Abajo FJ. Spatial Nonlocality in the Optical Response of Metal Nanoparticles. J. Phys. Chem. C. 2011; 115:19470–19475.
10. Fuchs R, Claro F. Multipolar response of small metallic spheres: Nonlocal theory. Phys. Rev. B. 1987; 35:3722–3727.
11. Boardman, AD. Electromagnetic Surface Modes. John Wiley & Sons Ltd; 1982.
12. Supplementary Materials.
13. Toscano G, Raza S, Jauho A-P, Mortensen NA, Wubs M. Modified field enhancement and extinction by plasmonic nanowire dimers due to nonlocal response. Opt. Express. 2012; 20:4176–4188. [PubMed: 22418175]
14. Zuloaga J, Prodan E, Nordlander P. Quantum Description of the Plasmon Resonances of a Nanoparticle Dimer. Nano Lett. 2009; 9:887–891. [PubMed: 19159319]
15. Marinica DC, Kazansky AK, Nordlander P, Aizpurua J, Borisov AG. Quantum Plasmonics: Nonlinear Effects in the Field Enhancement of a Plasmonic Nanoparticle Dimer. Nano Lett. 2012; 12:1333–1339. [PubMed: 22320125]
16. Esteban R, Borisov AG, Nordlander P, Aizpurua J. Bridging quantum and classical plasmonics with a quantum-corrected model. Nature Communications. 3:825–859. (1AD).
17. Hill RT, et al. Leveraging Nanoscale Plasmonic Modes to Achieve Reproducible Enhancement of Light. Nano Lett. 2010; 10:4150–4154. [PubMed: 20804206]
18. Decher G. Fuzzy nanoassemblies: Toward layered polymeric multicomposites. Science. 1997; 277:1232–1237.
19. Bain C, et al. Formation of Monolayer Films by the Spontaneous Assembly of Organic Thiols From Solution Onto Gold. J. Am. Chem. Soc. 1989; 111:321–335.
20. Wallwork M, Smith D, Zhang J, Kirkham J, Robinson C. Complex chemical force titration behavior of amine-terminated self-assembled monolayers. Langmuir. 2001; 17:1126–1131.
21. Sardar R, Shumaker-Parry JS. Asymmetrically functionalized gold nanoparticles organized in one-dimensional chains. Nano Lett. 2008; 8:731–736. [PubMed: 18269261]
22. Tronin A, Lvov Y, Nicolini C. Ellipsometry and X-Ray Reflectometry Characterization of Self-Assembly Process of Polystyrenesulfonate and Polyallylamine. Colloid. Polym. Sci. 1994; 272:1317–1321.
23. Jewsbury P. Electrodynamic Boundary-Conditions at Metal Interfaces. J. Phys. F: Met. Phys. 1981; 11:195–206.
24. Aubry A, Lei DY, Maier SA, Pendry JB. Plasmonic Hybridization between Nanowires and a Metallic Surface: A Transformation Optics Approach. ACS Nano. 2011; 5:3293–3308. [PubMed: 21361306]
25. Johnson PB, Christy RW. Optical Constants of the Noble Metals. Phys. Rev. B. 1972; 6:4370–4379.

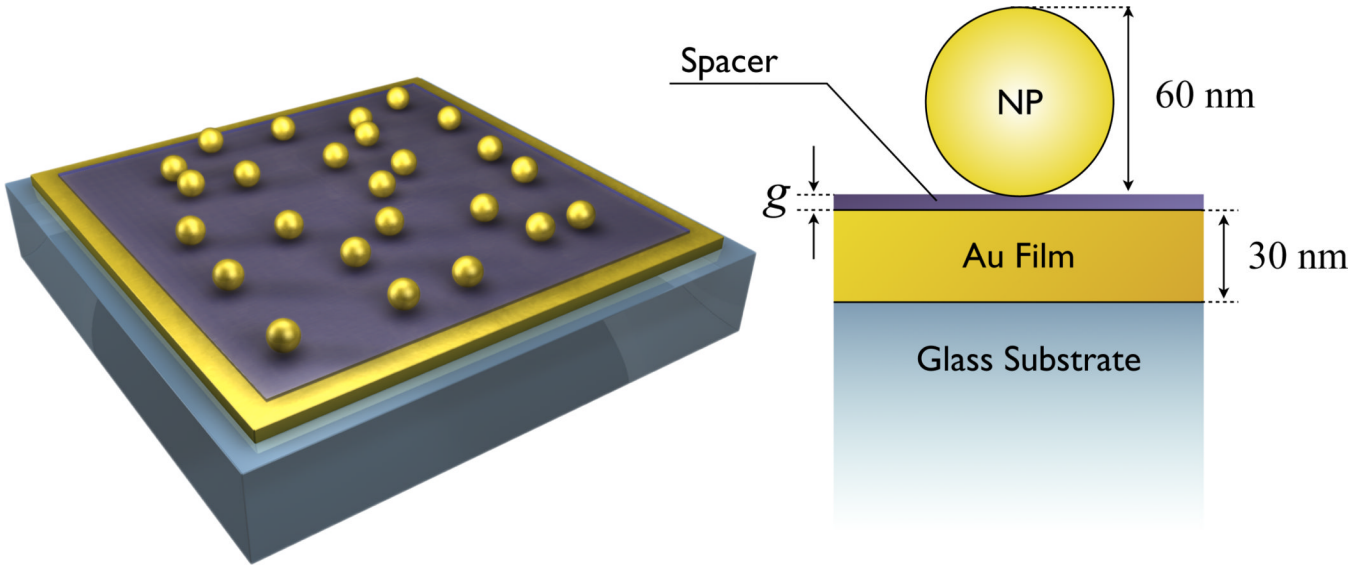

Fig. 1.
Geometry of the film-coupled nanoparticle. **Left:** Schematic of the sample. **Right:** Cross-section of a single film-coupled nanosphere.

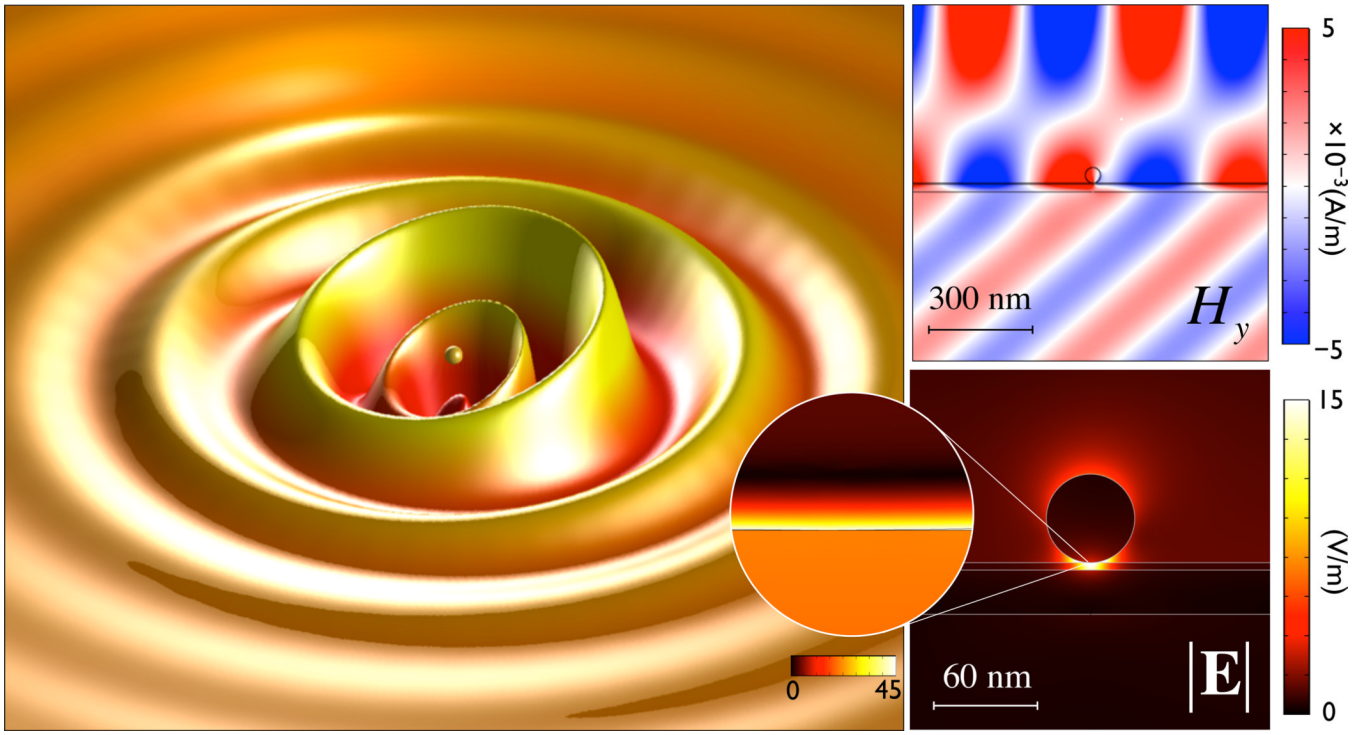

Fig. 2.

Simulation of a single film-coupled nanoparticle. **Left**: Relative electron surface density showing the exited surface plasmon polariton propagating over the metal film. **Right** (top): A plane wave is incident at 75° from normal on the nanoparticle. **Right** (bottom): A close-up of the near-fields surrounding the nanosphere; note the large field amplitude directly below the sphere. Looking closer yet, it can be seen that the fields penetrate into the nanosphere a distance on the order of the Thomas-Fermi screening length.

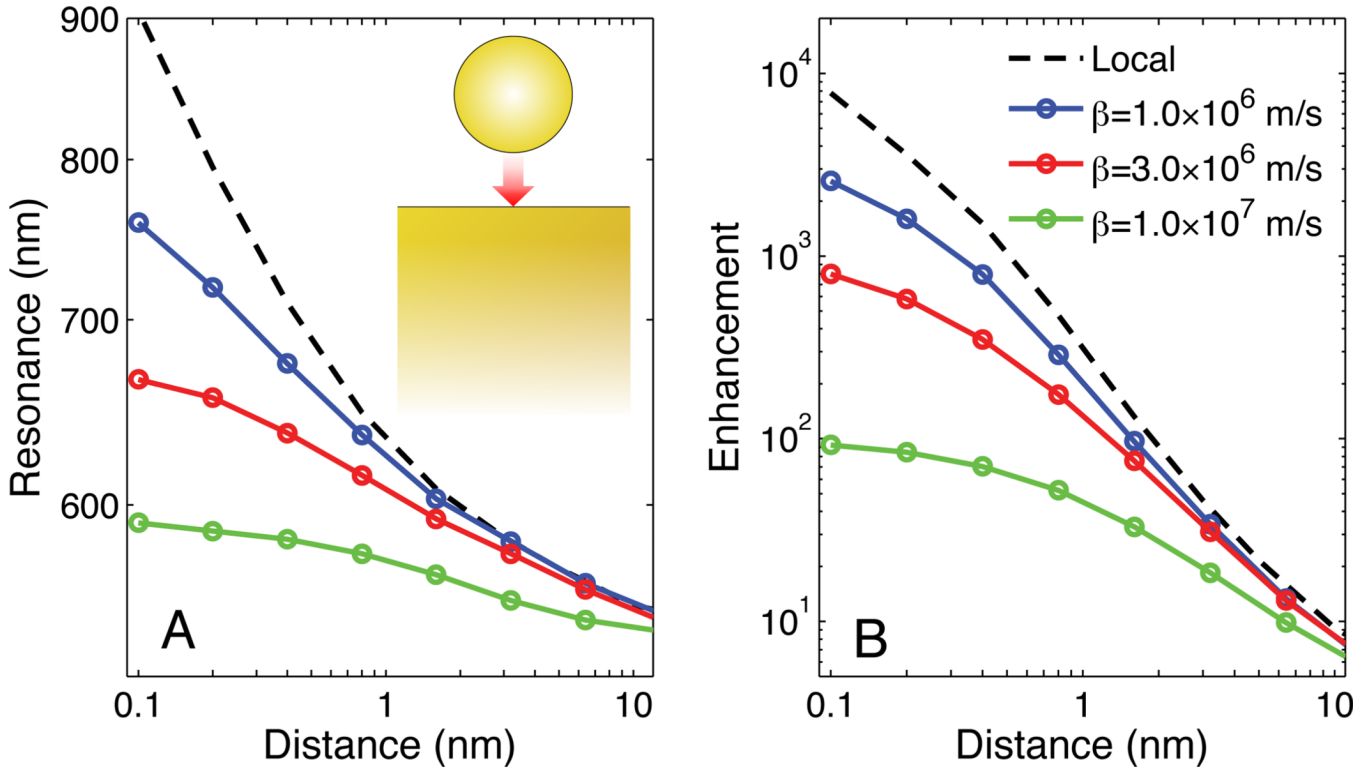

Fig. 3.

Behavior of the film-coupled nanosphere, assuming a local model and the nonlocal model with various values of β, as a function of gap distance. Calculations refer to a gold nanosphere of radius r = 30nm on a 300 nm thick film. (**A**) Position of the peak scattering intensity as a function of gap distance. (**B**) The corresponding field enhancement ratio. Note that in the absence of nonlocal effects, the peak scattering wavelength is extreme and the field enhancement grows to enormous values; nonlocality places a limit on the ultimate enhancement.

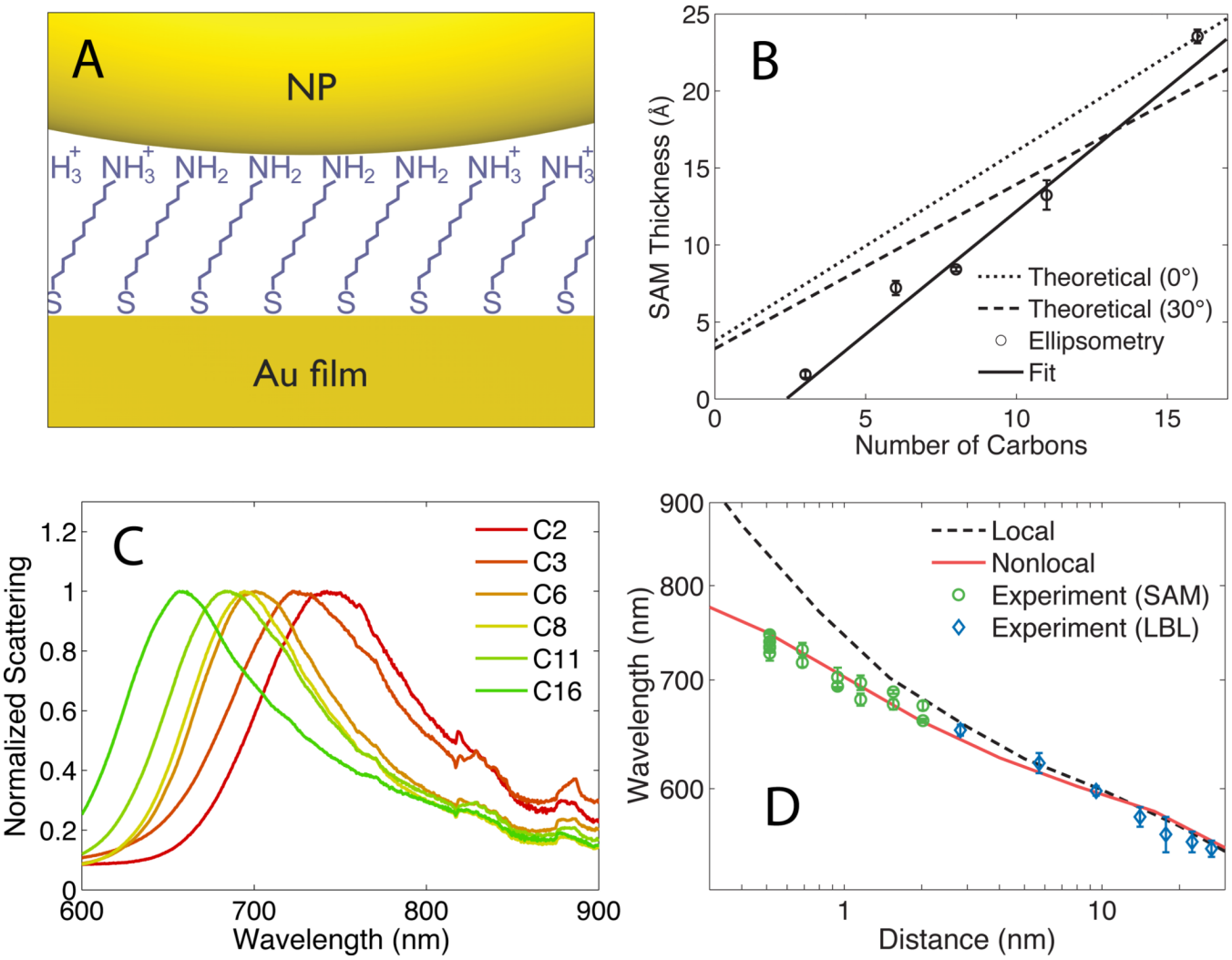

Fig. 4.

Experimental confirmation of nonlocal contributions to surface plasmon scattering. (**A**) Schematic of NP-film gap system showing a gold NP separated from the film by an amine-terminated alkanethiol SAM. (**B**) Thickness of the SAM layers as a function of the number of carbon atoms. (**C**) Normalized dark-field measured spectra of ensembles of film-coupled NPs for SAM spacer layers of different numbers of carbon atoms. (**D**) Comparison of experimental measurements from both SAM and LBL type spacers with numerical results with $\beta = 1.27\times10^{6}$m/s.